5G Communication with a Heterogeneous, Agile Mobile Network in the Pyeongchang Winter Olympic Competition

Grant agreement n. 723247

Deliverable D3.2
Electronically Reconfigurable Antenna Arrays for Backhauling & Fronthauling

Date of Delivery:	31 August 2017 (Contractual)	02 October 2017 (Actual)
Editor:	Antonio Clemente (CEA)	
Associate Editors:	Giuseppe Destino (Univ. Oulu)	
Authors:	Antonio Clemente (CEA), Maciej Smierzchalski (CEA), Marko Sonkki (Univ. Oulu), Marko Leinonen (Univ. Oulu), Giuseppe Destino (Univ. Oulu)	
Dissemination Level:	PU	
Security:	Public	
Status:	Final	
Version:	V1.0	
File Name:	5GCHAMPION_D3.2_Final.pdf	
Work Package:	WP3	

	Title:	Deliverable D3.2: Electronically reconfigurable antenna arrays for backhauling and fronthauling
	Date: 02-10-2017	**Status: Final**
	Security: PU	**Version: V1.0**

Abstract

This deliverable presents the design, optimization and preliminary experimental results of the two antenna solutions, (i) electronically steerable transmitarray and (ii) electrically large phased array, developed in the 5GCHAMPION project and used to implement the backhaul link.

Index terms

Antenna for backhauling, mmWave backhauling, electronically steerable antennas, 5GCHAMPION, 5G antennas, beamforming, beam-steering, transmitarray, phased array.

Contents

Table of Figures

1 Introduction

The WP3 is the largest WP of the 5GCHAMPION project comprising of 10 partners (5 in the Europe and 5 in the Korea). In Europe, the University of Oulu, Nokia and CEA are the partners with the largest amount of PM. In Korea, HFR and ETRI are the dominant partners.

The main activities in WP3 focus on:

- The development of mmW backhaul for the 5GCHAMPION proof-of-concept at the Winter Olympics,
- The study as well as development of algorithms, channel model and mobility management methods for a high-speed train (HST) (500km/h) use-case.

WP3 comprises of 4 R&D tasks, namely,

- T3.1: Advanced Antenna Arrays and RF front-end platform for mmW Backhauling & Fronthauling,
- T3.2: Algorithms for backhauling & fronthauling,
- T3.3: Implementation and testing of the mmWave backhaul/fronthaul transceiver platform,,
- T3.4: Mobility management.

Tasks T3.1, T3.2 and T3.3 are designed for the development of a 5G mmW backhaul, whereas T3.2 and T3.4 for the high speed use-case scenario.

This deliverable presents a part of the activity developed in the T3.1. In particular, the design, optimization and preliminary experimental results of the two antenna solutions, (i) electronically steerable transmitarray and (ii) electrically large phased array, developed in the 5GCHAMPION project and used to implement the backhaul link will be presented.

The document is organized in two main parts, one for each antenna technology. General conclusions and perspective are provided at the end of the report.

2 Electronically steerable transmitarray antenna

In this chapter, the realized electronically reconfigurable transmitarray with analogue beamforming capability is presented and its preliminary performances described. All the antenna blocks are also presented and characterized considering specific measurement setups. A 400-element array has been optimized and simulated used an ad-hoc tool previously developed at CEA-Leti. The antenna has been fabricated and its characteristics will be presented in the deliverable D3.3 (*Beamforming-antennas and front-end integration*). The full transmitarray simulation results will be presented. The proposed antenna is based on the previous demonstrations developed at CEA-Leti [1]-[4]. In particular, the 1-bit linearly-polarized tunable unit-cell proposed in [3] has been successfully optimized in a large bandwidth 24 – 30 GHz in order to cover both the European (800 MHz in the band 26.5 – 29.2 GHz) and the Korean (1 GHz in the 24.25 – 27.5 GHz band) frequency bands.

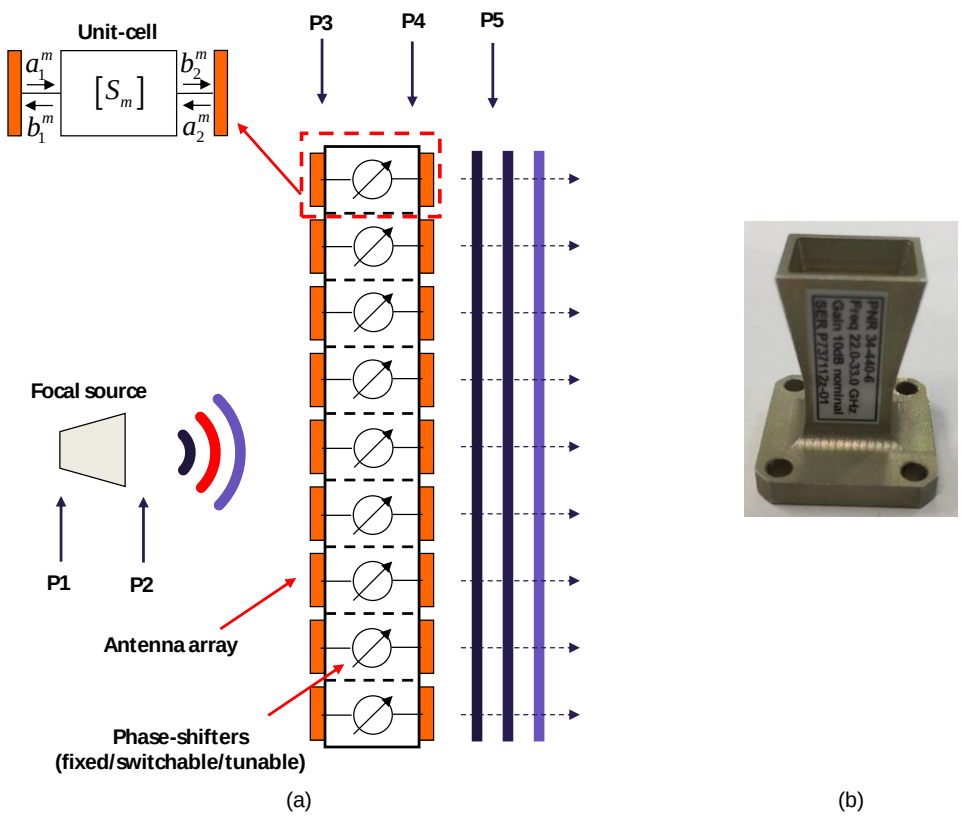

Figure 1: Electronically steerable transmitarray. (a) Schematic view and (b) photograph of the ATM 34-440-6 standard gain horn with 10 dBi nominal gain used as focal source.

2.1 Transmitarray antenna description and specifications

A transmitarray antenna (see schematic view in Figure 1) can be easily realized using standard printed circuit board (PCB) technologies and is typically composed of a focal source illuminating a multi-layer dielectric/metallic flat-array of elements or unit-cells. The transmission phase of each unit-cell is electronically controlled by integrating tunable elements such as PIN diodes, varactors or RF-MEMS in order to implement a given phase compensation and steer the

radiated beam in a given direction. Thanks to the used spatial feeding mechanism, which can drastically reduce the power losses on the array feeding network, transmitarray is an excellent antenna solution at millimeter wave frequencies compared to classical phased array. Furthermore, the beam-steering capability is easily implemented by integrating tunable devices on the flat-array aperture without using complex phase-shifter devices.

Thanks to their electronically tunable capability, the proposed flat-lens array could be easily interfaced and fed with different type of focal sources (e.g. standard gain horn antennas, small arrays, etc.). In order to simplify the validation phase, the transmitarray has been characterized by using as a focal source the ATM 10-dBi standard gain horn presented in Figure 1(b). The proposed antenna specifications are listed below.

- Operational frequency band: 24 – 30 GHz,
- Polarization: simple linear,
- Scanning capability: 2D window of ±40°,
- Minimum gain: > 20 dBi.

One important parameter in the design of transmitarray antennas is its tunable phase range. In the ideal case, the transmission phase of each unit-cell must be tuned in the continuous range 0:360°. In practice, phase quantization is introduced in order to make a trade-off between unit-cell and tunable device polarization network complexity, cost, required bandwidth, and insertion losses. In this case, a 1-bit phase quantization (two phase states 0° and 180°) is selected.

2.2 Design, optimization and characterization of the tunable unit-cell element

The proposed 1-bit tunable unit-cell architecture is presented in Figure 2(a) and consists of four metal layers, two identical substrates of Rogers Duroid RT6002 and one bonding film of Arlon CuClad 6700. The receiving layer (labeled as passive patch antenna) is composed of a rectangular patch loaded by a U-shaped slot, while the transmitting layer (labeled as active patch antenna) contains a rectangular patch loaded by an O-shaped slot and the two PIN diodes. In the electromagnetic (EM) simulator, these active devices are modelled as a lumped-element equivalent circuit extracted from the measurements (Figure 2(b)) and a gallium-arsenide block (Figure 2(c)) [3]. This active patch is connected to the passive one with a metallized via hole placed at the center of the unit-cell. A ground plane occupies one of the two intermediate layers. The other inner layer contains the biasing lines.

In the proposed unit-cell structure, one PIN diode is biased in the forward state with a 10-mA current. The 1.3-V threshold voltage of this diode is sufficient to maintain the other diode, mounted in anti-parallel configuration, in its reverse state. Thus, only one bias line is necessary for each unit-cell, facilitating thereby the layout and routing of the bias network in very large array configurations. The bias line is 100-μm wide and is connected to the active patch by using two symmetric metallic via connections. More details on the 1-bit unit-cell operational principle, model, parametric analysis, and simulation setup are detailed in [3].

PIN diodes (MA4AGP907 from M/ACOM [5]) have been selected as active devices for their low insertion losses and small size (see geometrical characteristics presented in Figure 2(c)). A series L-R circuit (R_{ON} = 4.2, L_{ON} = 0.05 nH) and a shunt R-C circuit (R_{OFF} = 300 k, C_{OFF} = 42 fF) are used in the 3D electromagnetic simulation as model for the two states, respectively. These values have been extracted from measurements and full-wave simulations as presented in [6].

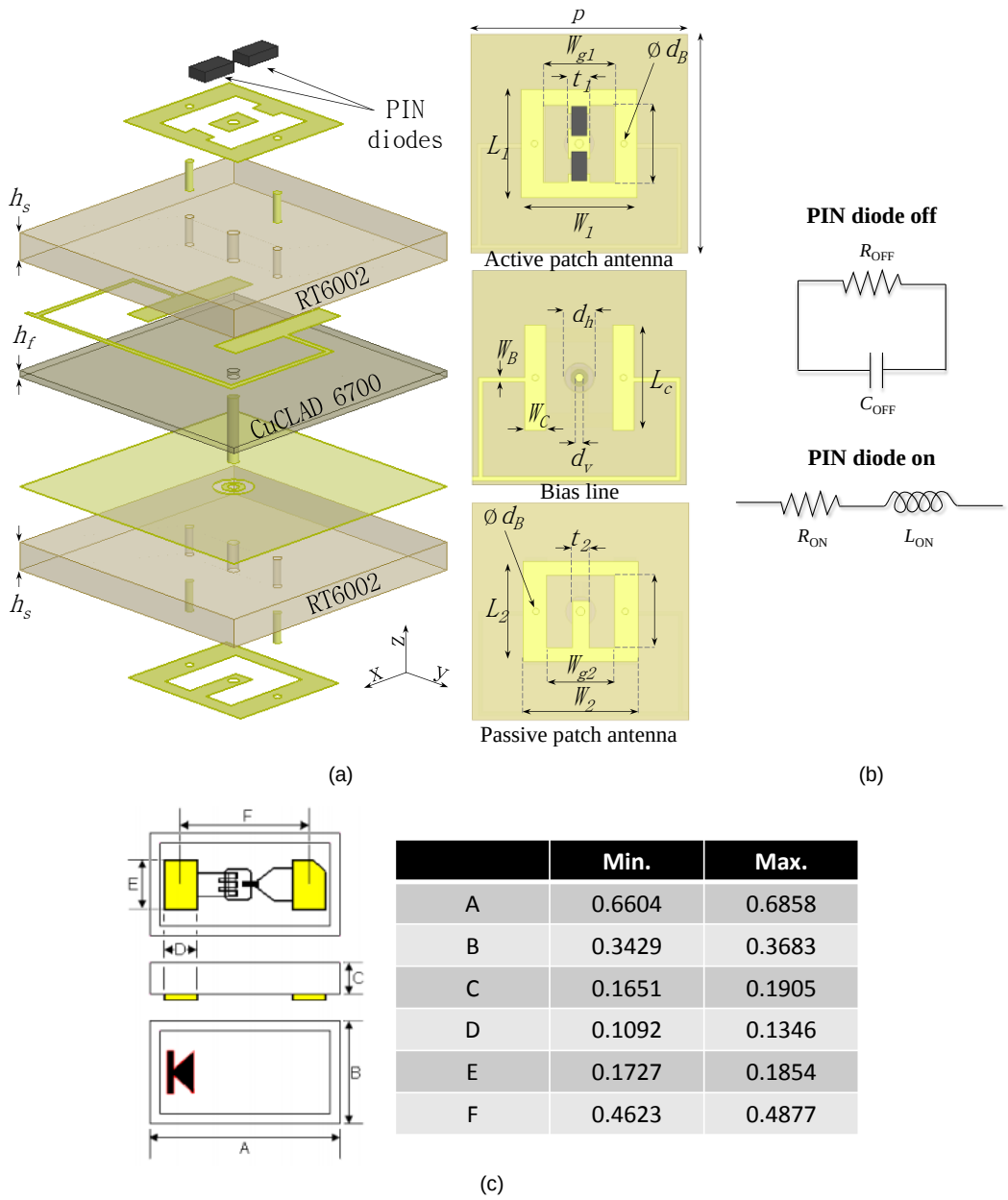

	Min.	Max.
A	0.6604	0.6858
B	0.3429	0.3683
C	0.1651	0.1905
D	0.1092	0.1346
E	0.1727	0.1854
F	0.4623	0.4877

Figure 2: Electronically tunable 1-bit unit-cell with integrated PIN diodes. (a) Schematic view and stack-up, (b) equivalent lumped element model of the PIN diodes, and (c) PIN diodes geometrical characteristics.

2.2.1 Simulation and optimization of the unit-cell

The unit-cell has been simulated using the commercial software Ansys HFSS considering periodic boundary conditions and Floquet port excitations to take into account the mutual couplings with the surrounding unit-cells (Figure 3). The full-wave simulations under normal incidence give the scattering parameters calculated for the two phase states (Figure 4).

The simulated minimum insertion loss is only 0.61 dB at 30 GHz with a 3-dB transmission bandwidth of 23.6 – 30 GHz (23.7% @ 27 GHz) for the unit-cell state 0° and 23.8 – 31.1 GHz (26.9% @ 27 GHz) for the unit-cell state 180°. The phase difference between the two states is around 180° on the whole frequency band. The 1-bit unit-cell bandwidth performances are synthetized in Table 1 as a function of the phase state (0° and 180°).

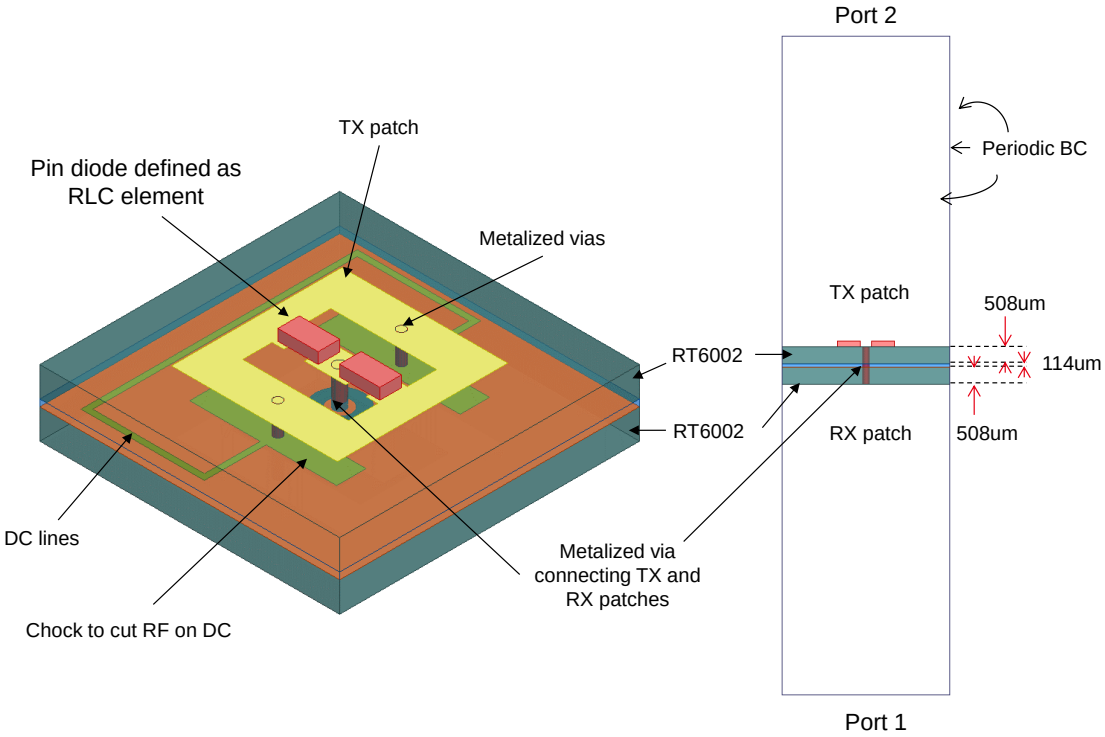

Figure 3: Simulation setup of the 1-bit electronically tunable unit-cell.

Unit-cell	Insertion Loss (dB)	-2 dB Bandwidth (% @ 27 GHz)	-3 dB Bandwidth (% @ 27 GHz)
0°	0.99	22.9	23.7
180°	0.61	25.5	26.9

Table 1: Synthesis of the linearly-polarized electronically tunable unit-cell performances.

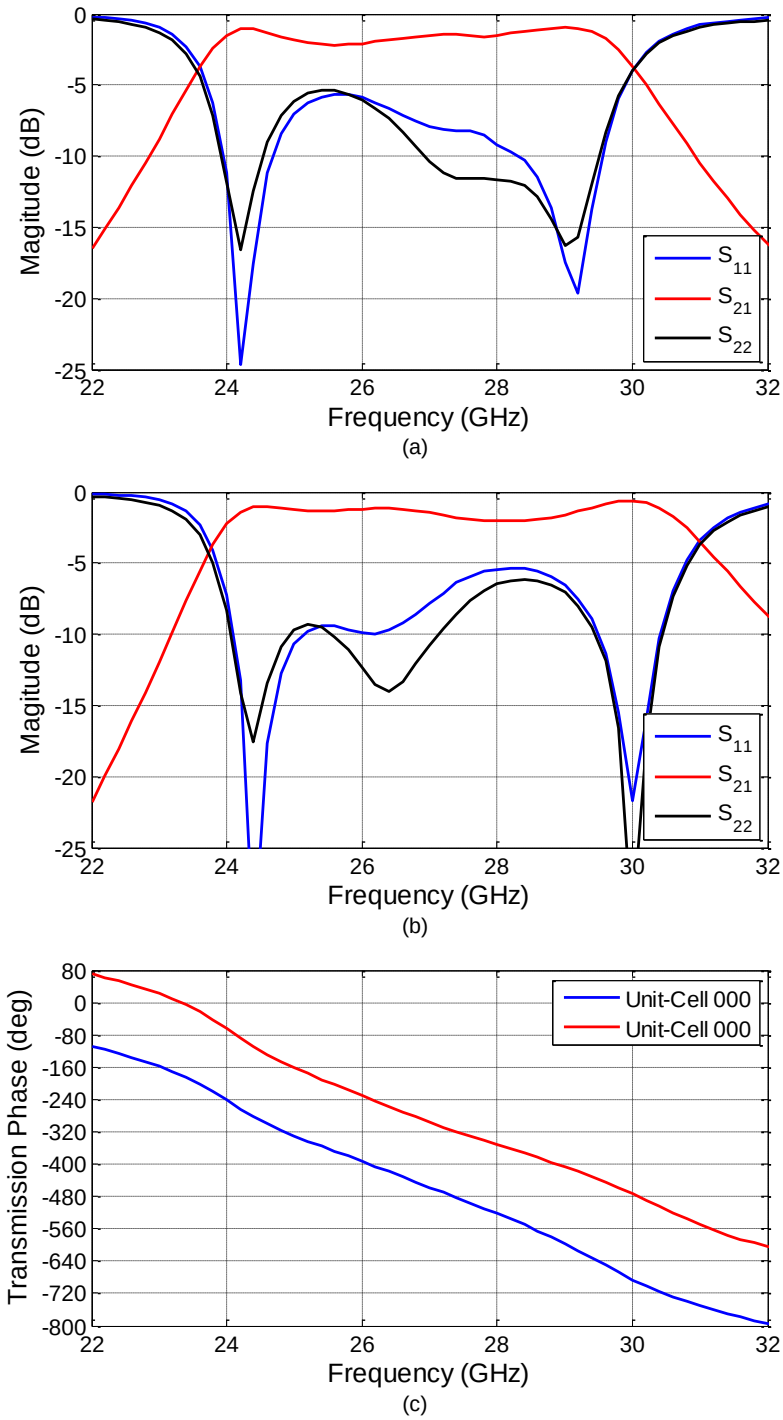

Figure 4: Simulated scattering parameters of the 1-bit electronically tunable unit-cell. (a) Amplitude of the transmission and reflection coefficients of the unit-cell 0°, (b) amplitude of the transmission and reflection coefficients of the unit-cell 180°, and (c) transmission phase.

2.2.2 Fabrication and experimental characterization of the unit-cell

The unit-cell has been fabricated (Figure 5) and characterized in a waveguide simulator (Figure 6) based on standard WR-28 waveguides (7.112×3.556 mm^2). It is formed by two coax-to-WR-28 adaptors, two WR-28 straight waveguide sections and two tapered transitions between the rectangular section of the waveguides and the square section of the unit-cell; these transitions have an optimized length of 1.2 mm (λ_0/8.6) to minimize the impedance mismatch (Figure 6(c)).

The realized prototype of the unit-cell is shown in Figure 5. The original design is surrounded by two rings (6×6mm^2 and 9×9mm^2) of metallized vias with a diameter of 500 µm. These rings associated with the metallic areas in contact with the WR-28 flanges warranty the continuity of the waveguide walls and avoid the propagation of substrate modes outside the unit-cell. Two bias lines, passing through the two rings of vias, and pads for the ground connections are included on the boards. Further full-wave simulation studies performed with the complete setup have shown their negligible impact on the frequency response of the unit-cell. As announced before, this prototype has been tested in the waveguide simulator shown in Figure 6. In order to de-embed the waveguide sections and coax-to-waveguide adaptors from the unit-cell scattering parameters, a TRL calibration with waveguide standards has been performed. The two thin ad-hoc transitions from the WR-28 sections to the square unit-cell sections are not de-embedded. Indeed, the unit-cell section (5.1×5.1 mm^2) does not allow the propagation of the fundamental TE10 mode at 29 GHz (its cut-off frequency is 29.4 GHz) so that the transitions cannot be included in the calibration process.

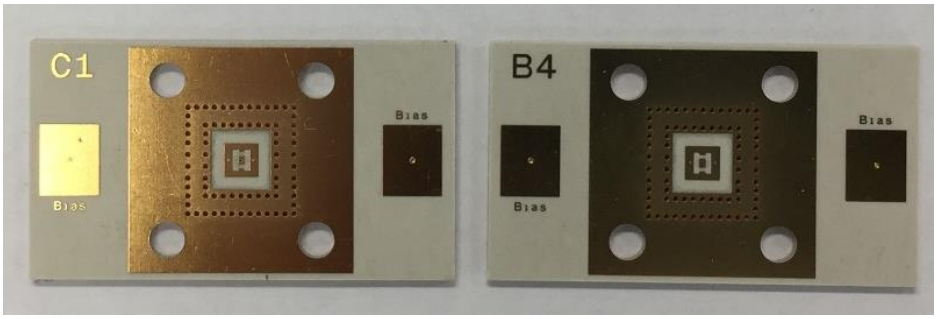

(a)

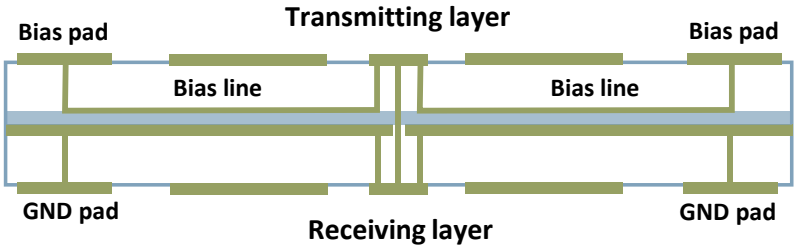

(b)

Figure 5: Electronically tunable unit-cell measurement setup in standard WR-28 waveguide. (a) Photograph of the full measurement setup, (b) zoom on the waveguide setup and (c) scheme of the waveguide setup.

The measured and simulated amplitude of the scattering parameters of the unit-cell obtained when the waveguide setup presented in Figure 6 is used are plotted in Figure 7 and in Figure 8 for the unit-cell 0° and 180°, respectively. A very good agreement has been obtained between simulated and experimental results when the same setup is considered. As expected, there is a difference between these results and the scattering parameters calculated with periodic boundary conditions and normal incidence. In particular, we can observe a 500-MHz shift towards lower frequencies. This is mainly due to the oblique incidence of the waves in the waveguide simulator [3],[6]. In the case of the standard rectangular waveguide WR-28 the equivalent incidence angle is equal to 45°.

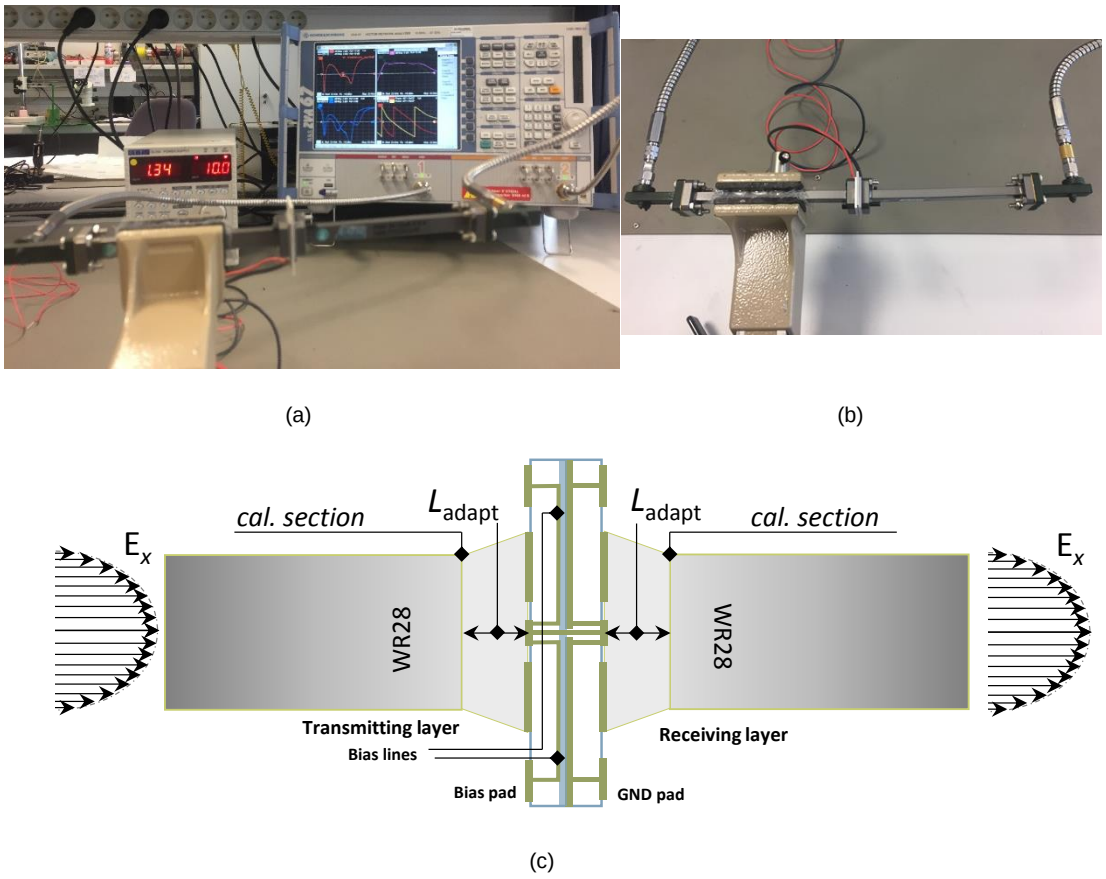

Figure 6: Electronically tunable unit-cell measurement setup in standard WR-28 waveguide. (a) Photograph of the full measurement setup, (b) zoom on the waveguide setup and (c) scheme of the waveguide setup.

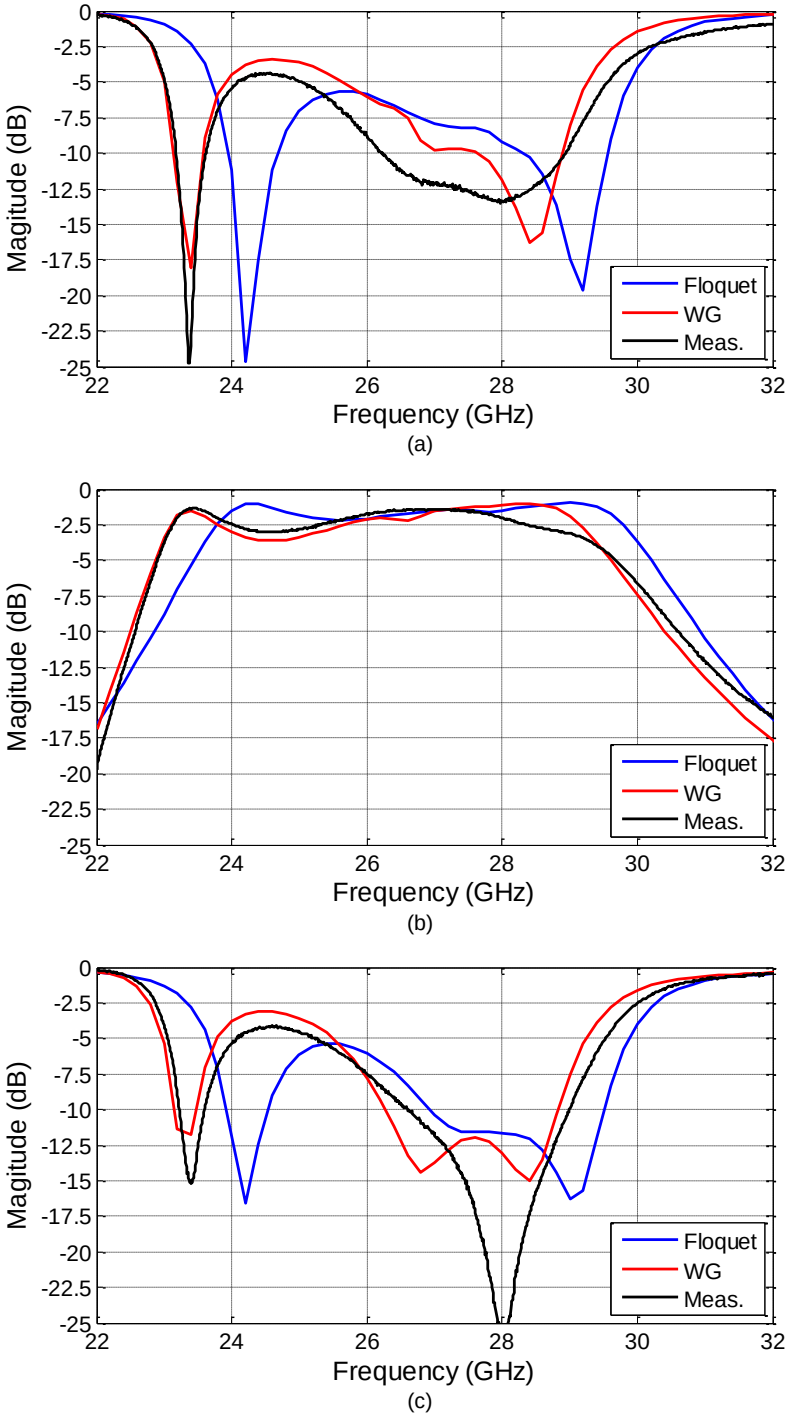

Figure 7: Simulated and measured scattering parameters of the 1-bit electronically tunable unit-cell 0°. (a) Amplitude of the reflection coefficients S_{11}, (b) amplitude of the transmission coefficients, and (c) amplitude of the reflection coefficients S_{22}.

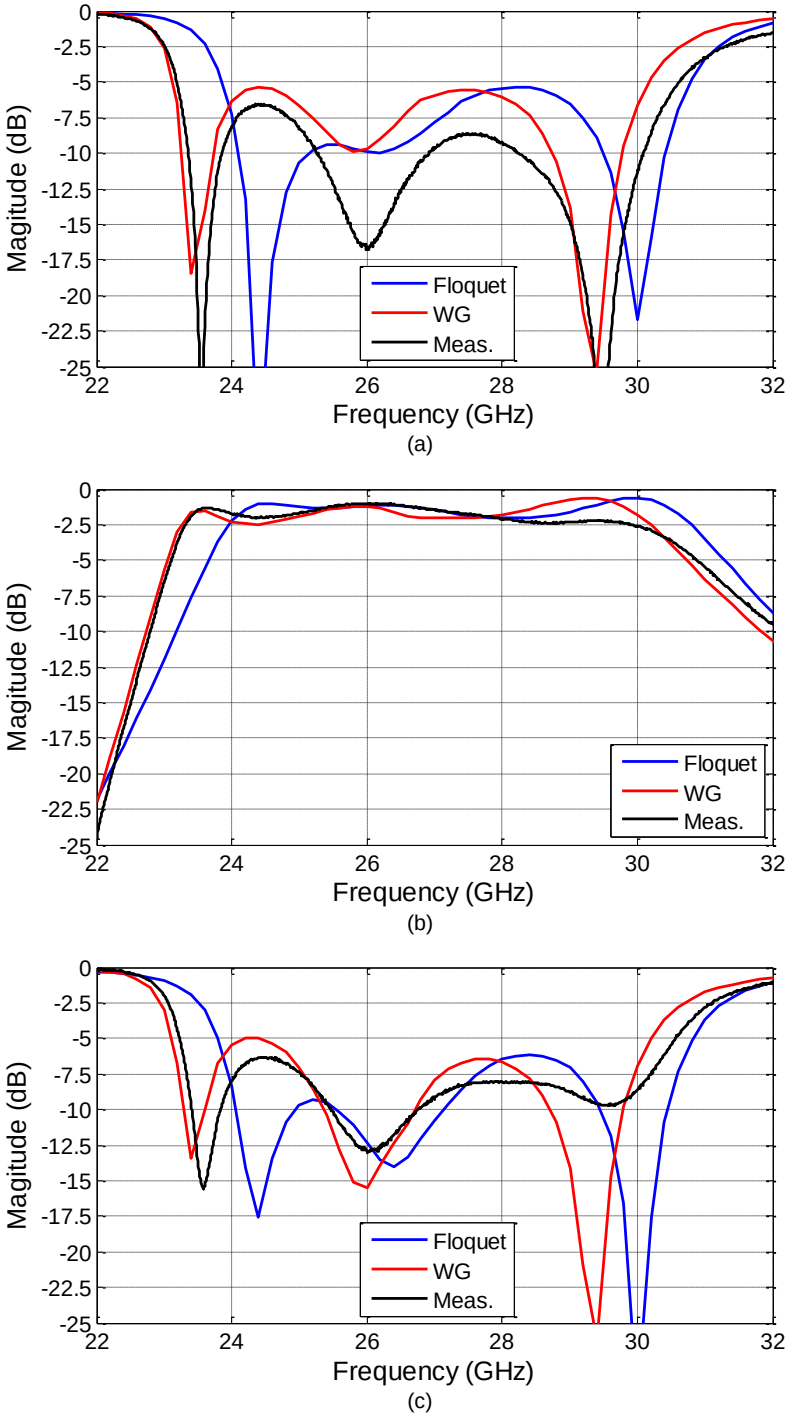

Figure 8: Simulated and measured scattering parameters of the 1-bit electronically tunable unit-cell 180°. (a) Amplitude of the reflection coefficients S_{11}, (b) amplitude of the transmission coefficients, and (c) amplitude of the reflection coefficients S_{22}.

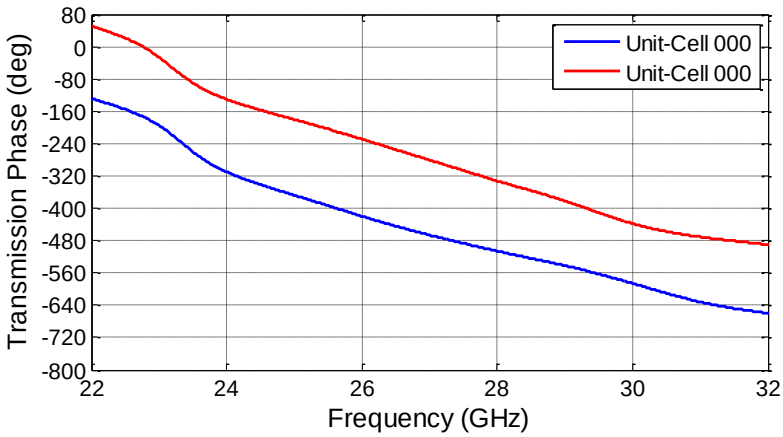

Figure 9: Measured transmission phase of the 1-bit electronically tunable unit-cell.

2.3 Design, optimization and fabrication of the linearly-polarized transmitarray

The schematic view of the proposed 1-bit electronically reconfigurable transmitarray with its steering logic is presented in Figure 10. The flat-lens array is composed of 400 linearly-polarized unit-cells with a total of 800 PIN diodes and is illuminated with the 10-dBi standard gain horn antenna. The flat-lens total size, including the 400 bias lines, are 196×196 mm². Four board-to-board connectors are also integrated to connect the array to the steering logic.

In order to select the diodes states of each unit-cell and implement the required phase distribution on the flat-lens aperture, a positive or a negative current must be applied on each bias line. Four control boards, whose dimensions are 150×150 mm² [2],[6] are used, one for each quarter of the transmitarray, which includes 100 unit-cells. Each board is formed by 13 shift registers and 25 4×4 switches. Chip resistors are used to obtained ±10 mA of current on each bias line at the output of the switches. The steering logic has been design only for the antenna characterization and cannot be used for real-time (beam-steering speed around 1-2 ms) steering purpose.

The total power consumption of the PIN diodes is about 5 W. The whole system, including the control boards, has a consumption of 20 W, due to the required voltage of the components used on these boards. The four boards are placed behind the focal plane and the connection with the antenna is realized with four ribbon cables. Using the ad-hoc control code, the programmable sequence is sent to each board serially. This data stream is saved on shift registers for a series-to-parallel conversion. Each switch is connected to a bias line of the transmitarray and gives a negative $-V_{cc}$ or positive V_{cc} voltage.

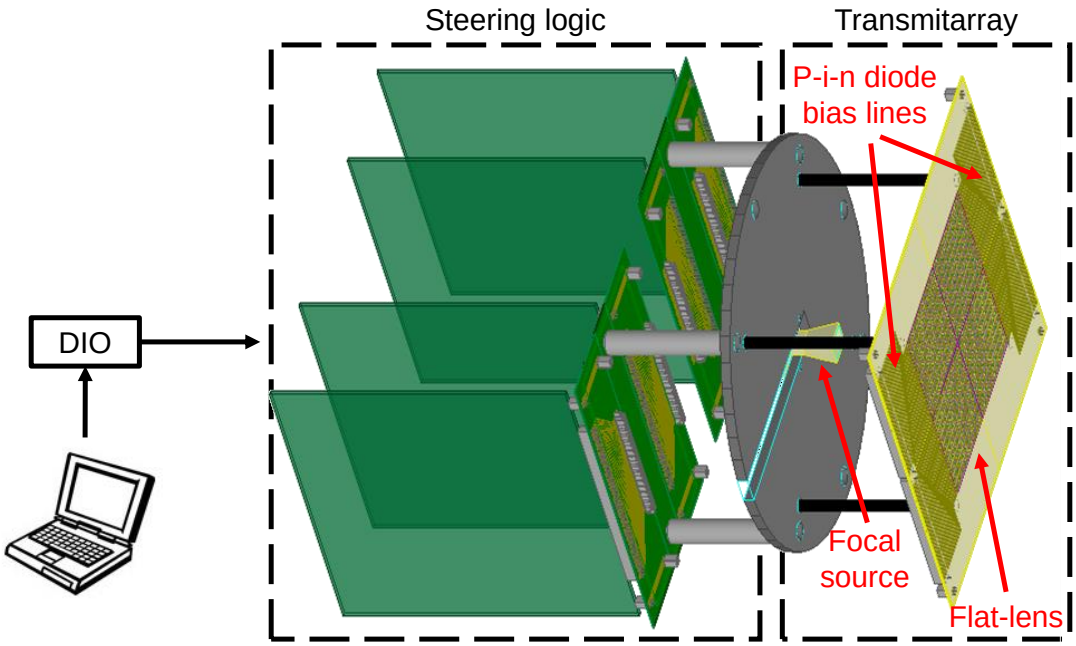

(a)

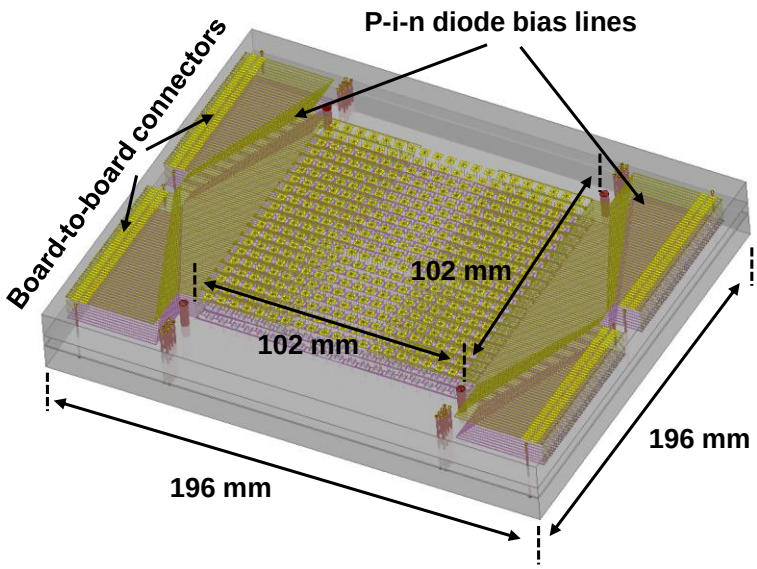

(b)

Figure 10: Schematic view of the 1-bit electronically reconfigurable transmitarray (a) including the steering logic and (b) 3D view of the realized 400-element flat-lens array.

2.3.1 Simulation and optimization of the transmitarray antenna

As previously discussed, the linearly-polarized unit-cell has been optimized in a large bandwidth 24 – 30 GHz in order to cover both the European (800 MHz in the band 26.5 – 29.2 GHz) and the Korean (1 GHz in the 24.25 – 27.5 GHz band) frequency bands. The distance *F* between the horn and the flat-lens array apertures is fixed to 60 mm in order to optimize the illumination taper and reduce the spill-over loss. The transmitarray optimization when the beam is directed in the broadside direction has been computed at three different frequencies, 26 (central frequency of the Korean band), 27 and 28 (central frequency of the European band) GHz, in order to reduce the impact of beam squint in three different frequency bands when the beam is electronically steered between -60° and 60°. The simulated maximum gains computed at the three different optimization frequencies is plotted in Figure 11 and Figure 12 as a function of the frequency and of the scan angle, respectively.

Finally, the gain radiation patterns computed for different scan angles and at the three optimization frequencies are plotted in Figure 13.

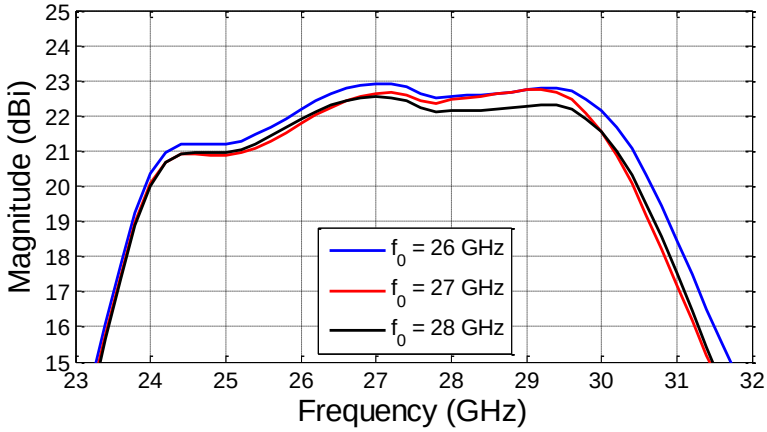

Figure 11: Simulated frequency response (broadside gain) of the 1-bit electronically reconfigurable transmitarray as a function of the optimization frequency.

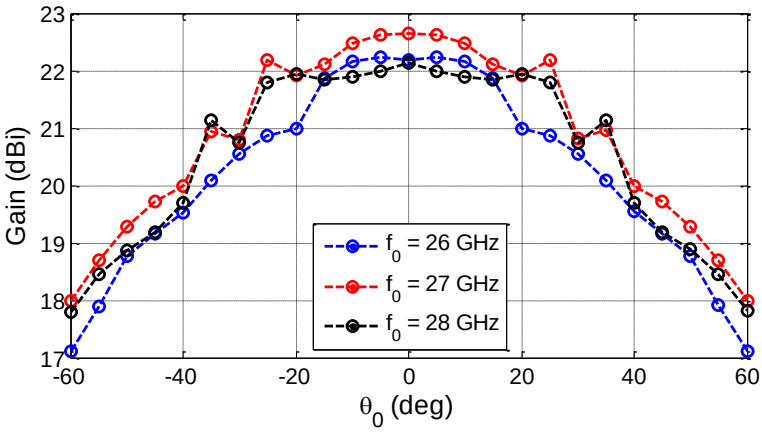

Figure 12: Simulated maximum gain of the 1-bit electronically reconfigurable transmitarray as a function of the optimization frequency and steering angle.

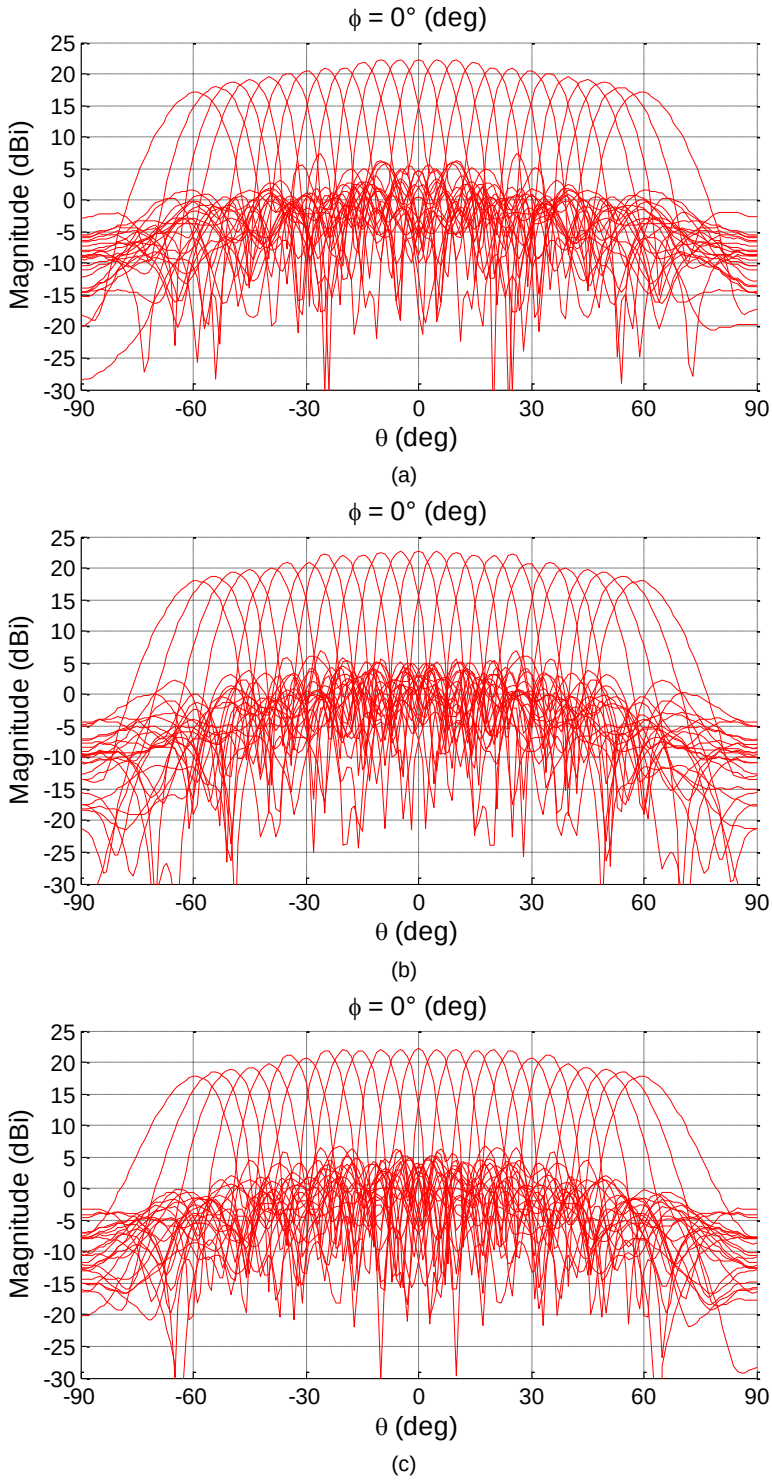

Figure 13: Simulated radiation patterns of the 1-bit electronically reconfigurable transmitarray compute at the optimization frequencies (a) 26, (b) 27, and (c) 28 GHz as a function of the scan angle.

2.3.2 Fabrication of the transmitarray antenna

In order to validate and verify the correct functionality of the steering logic the setup presented in Figure 14 has been used. The four control boards are connected to a specific board with 800 LED diodes used to emulate the PIN diodes integrated on the flat-lens array.

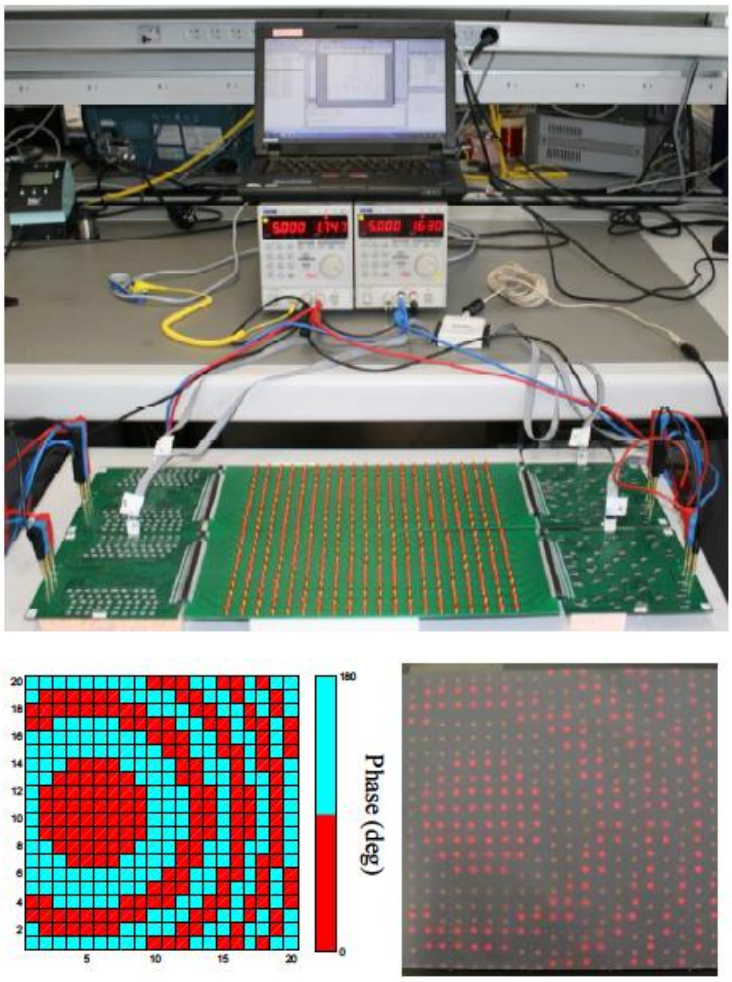

Figure 14: Validation setup of the steering logic and one example of desired and implemented 1-bit phase-shift distribution.

The fabricated linearly-polarized flat-lens and full transmitarray are presented in Figure 15. The measurement results of the radiation patterns will be presented in the future deliverable D3.3.

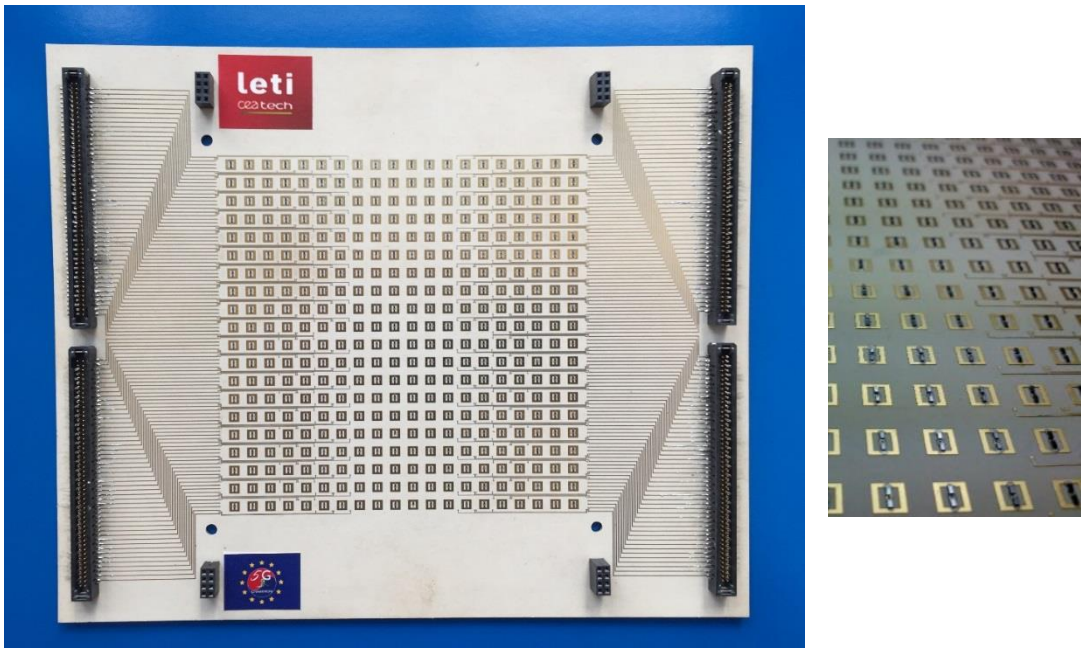

(a) (b)

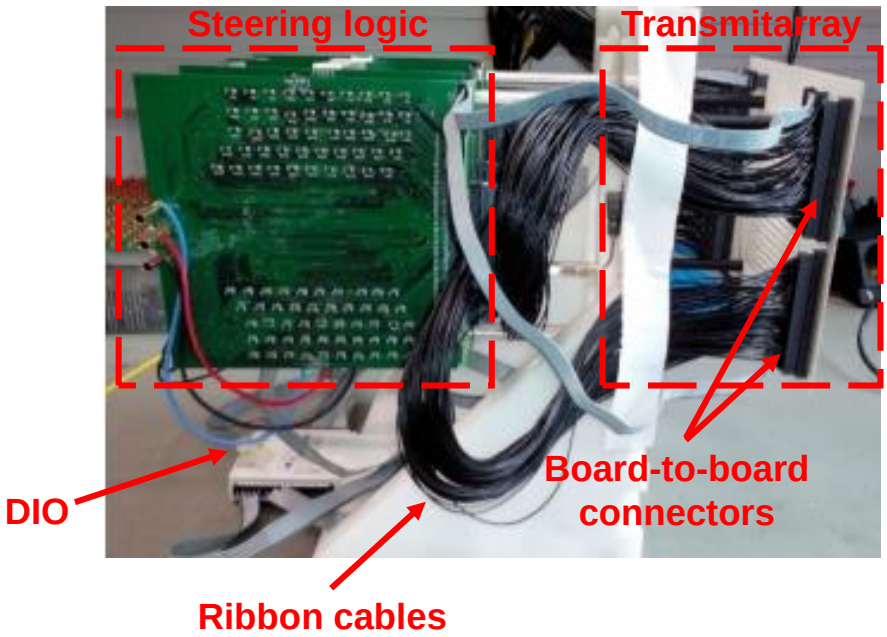

(c)

Figure 15: Fabricated electronically reconfigurable transmitarray antenna. (a) Flat-lens array, (b) zoom on the active layer with PIN diodes, and (c) view of the transmitarray with the focal source and the steering logic.

3 Electrically large antenna array for MIMO beamforming

This chapter describes the antenna array designed and developed for massive-MIMO demonstrator to operate at 28 GHz frequency range. The array consists of sub-arrays, which each has 2×2 element patch antennas. The sub-array is linearly-polarized and each patch element are excited with the same amplitude and equal phase. The total number of patch antennas in the massive-MIMO beamforming matrix is 4×16 elements, meaning 2×8 sub-arrays, and totally 64 elements. The presented simulation and measurement results are based on the Version 1, and, thus, the goal of the -10 dB impedance bandwidth was set to the 26.65 – 27.50 GHz, whereas the final version, Version 2, the goal is to fulfill the bandwidth from 24.25 to 29.20 GHz. The Version 2 also includes both ±45° polarization components.

3.1 Sub-array

This section presents the structure and the simulated results of the 2×2 element sub-array. A single sub-array is presented in Figure 10. The sub-arrays consists of four patches which are oriented in -45° polarization. The size of the sub-array is 10.8×10.8 mm^2 and the patch separation is half a lambda (= 5.4 mm) at 28 GHz. The metal cover is placed over the feed network to avoid backward radiation.

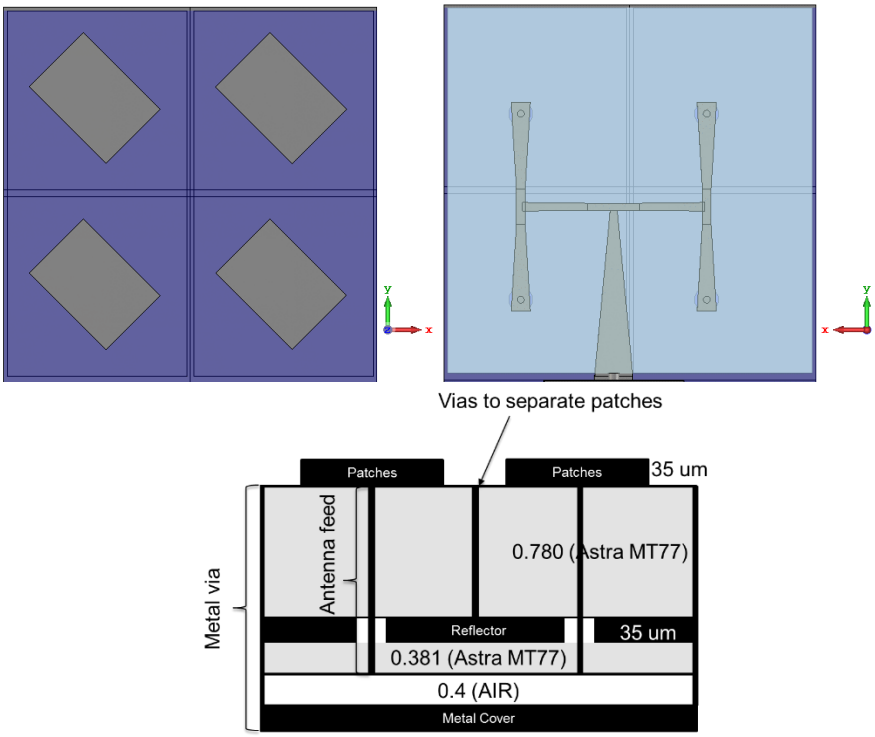

Figure 10: 2x2 element sub-array present in front with patches (left) and the feed network (right). Below is the cross section of the sub-array structure.

Figure 11 presents the simulated frequency response of the sub-array. As it can be observed, the simulated results show larger bandwidth potential as the required bandwidth with the Version 1, which is 26.65 – 27.50 GHz. At the aforementioned bandwidth, the sub-array shown approximately 90% total efficiency and the maximum realized gain at 27 GHz 10.40 dBi, as shown in Figure 12.

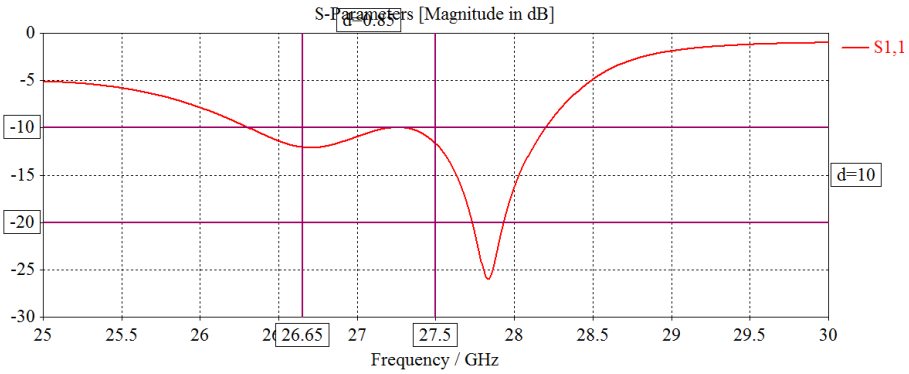

Figure 11: Simulated impedance of the single sub-array.

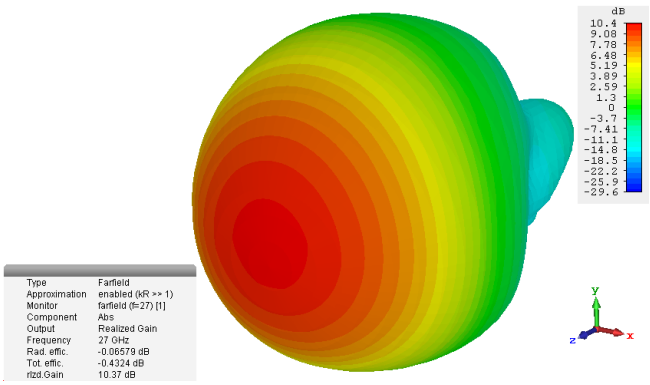

Figure 12: The radiation pattern of the single sub-array at 27 GHz.

3.2 Two Element Sub-Array Matrix (2x1)

This section presents an antenna matrix with two sub-arrays. This kind of setup can be seen as smallest combination of the sub-arrays in the antenna array as the purpose is not to use beamforming in the elevation plane. Figure 13 present the antenna structure with the simulated S-parameters. Both sub-arrays have the same feed network and cross section profile as presented in Figure 10. The both sub-arrays satisfy the -10 dB impedance bandwidth and the isolation between the antenna ports is better than 35 dB. Good isolation is corresponding to good polarization properties.

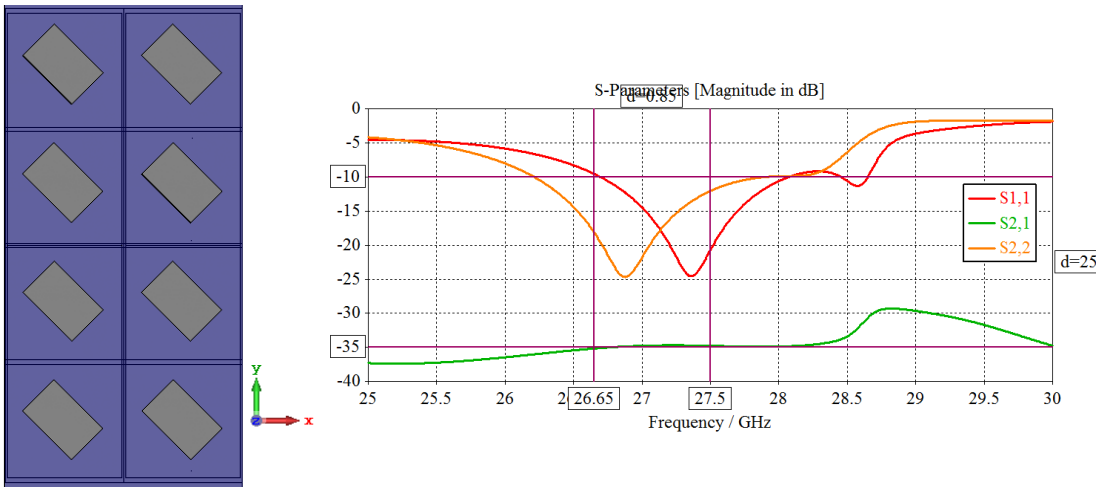

Figure 13: 2x1 matrix of sub-arrays (left), and the impedance matching and the mutual coupling (right). Size of the 2x1 array matrix is 21.6 x 10.8 mm².

Figure 14 presents the simulated 3D radiation pattern of the two element array. As it can be seen, the gain improve the 3 dB compared to the one sub-array case. The total efficiency is better than 87.5%. Sidelobe is slightly stronger in the direction of –Y and this is due to the fact that the feed network is not fully symmetrical as patches cannot be fed in the middle of the structure.

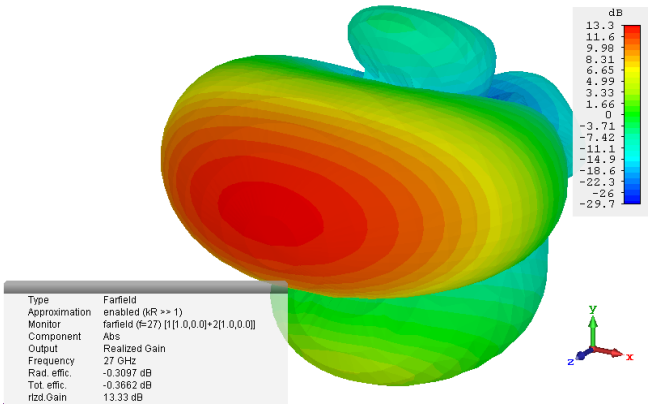

Figure 14: The radiation pattern of the 2x1 matrix of sub-arrays at 27 GHz.

3.3 2x8 Antenna Matrix

Figure 15 present the prototype of the 2×8 antenna matrix where are totally 16 sub-arrays. Thus, the total number of patch elements in the array matrix become 64 and the size of the array is 90 × 34 mm² (*W*x*L*). The structure is presented without SMPM-connectors and metal cover over the feed network.

The measured impedance matching of all the 16 ports are presented in the Figure 16. As it can be notice, the measured results are within the required bandwidth. The variation in the results is assumed to become from the manufacturing tolerances as simulations were predicting 50

µm changes in the structure has significant effect the performance. In the same figure, the measured mutual coupling between the selected ports are presented. It can be observed that the mutual coupling is smaller than -45 dB with adjacent elements. As a conclusion, when comparing the results in the Figure 13, simulations are well correlating with the measured ones.

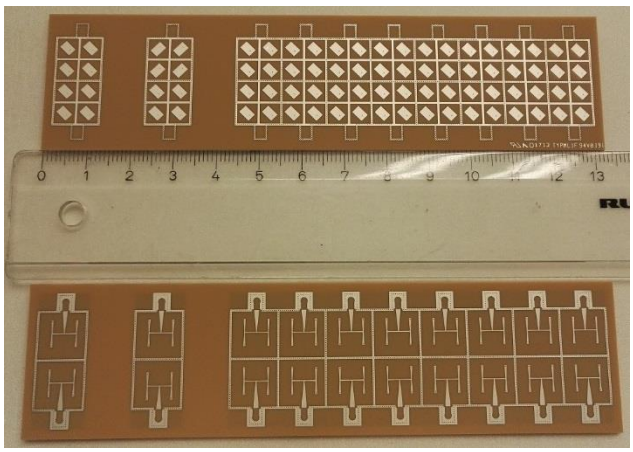

Figure 15: Photograph of the prototype antenna array. Above the antenna array is presented whereas below the one can see the feeding network. Two sub-arrays on the left side of the photograph are 2x1 sub-arrays for preliminary prototype tests. In the arrays matrix, the antenna ports are in the upper line from 1 to 8, from left to right, and the lower line from 9 to 16.

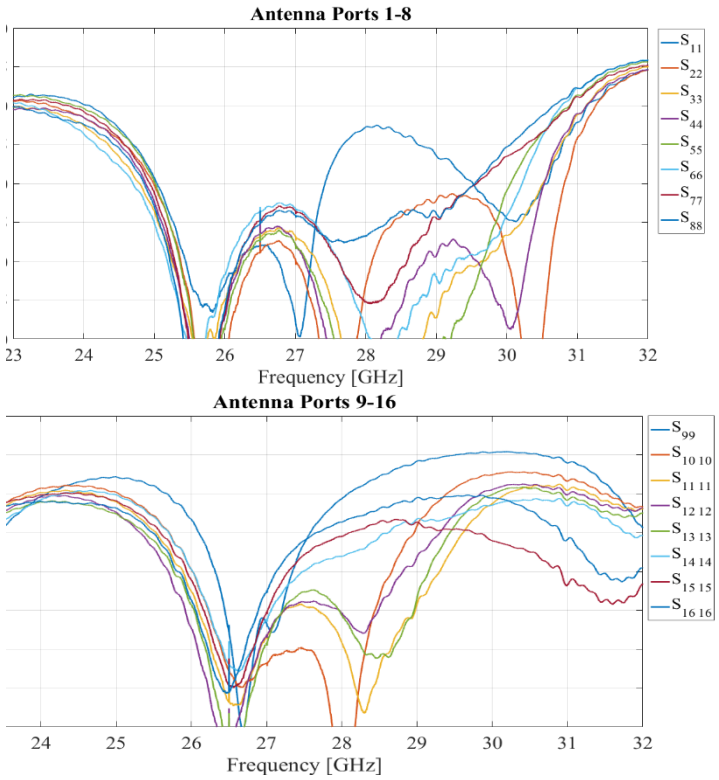

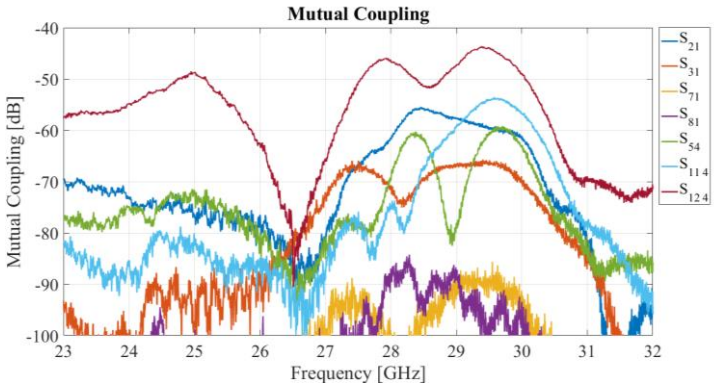

Figure 16: Measured impedance matches of the prototype antenna array. Upper present ports 1-8, the middle presents ports 9-16, and the lower one the mutual coupling between the selected ports.

Figure 17 presents the measured radiation patterns in azimuth plane (XZ-cut) at 26.50 GHz and 27.50 GHz. The radiation patterns are measured element by element and the results are summed in post-processing. Sidelobe level are 15 dB below the maximum gain which was predicted. The maximum gain is around 20 dBi as the theory is predicting max. 21.5 dBi so there is a good correlation between the results.

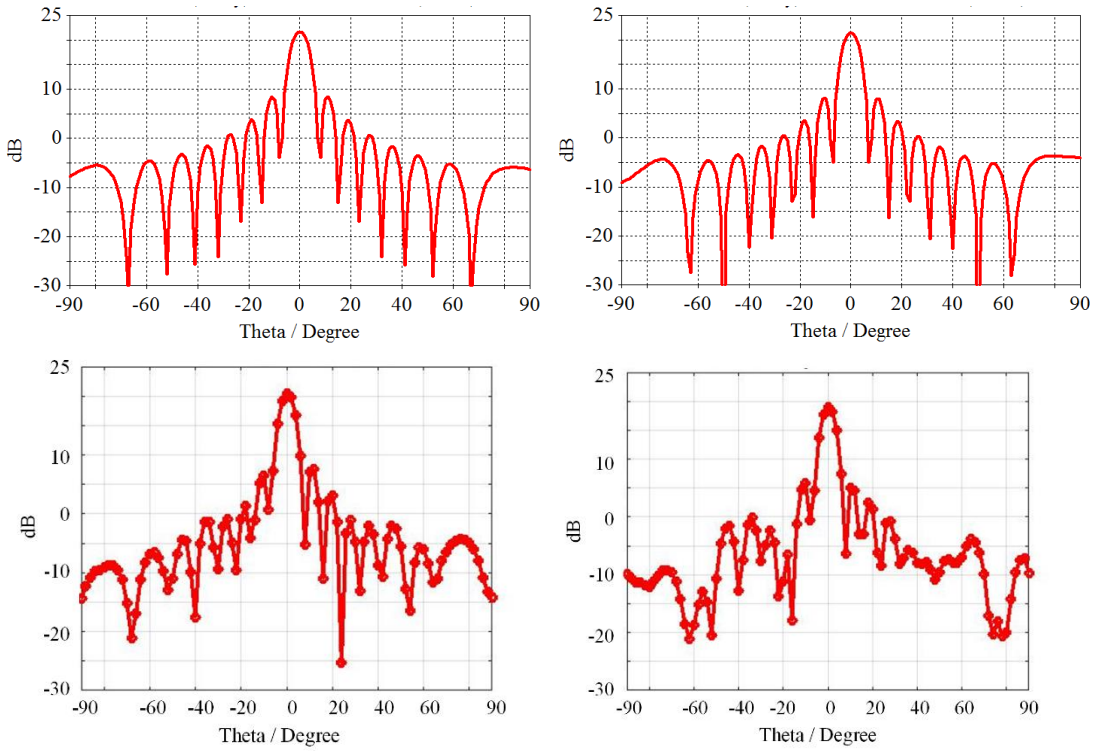

Figure 17: Simulated (up) and measured (down) radiation patterns of the array matrix in azimuth plane at 26.50 GHz and 27.50 GHz.

Figure 18 presents the radiation pattern measurement setup. The setup is still under construction but the currents results shows the system is running.

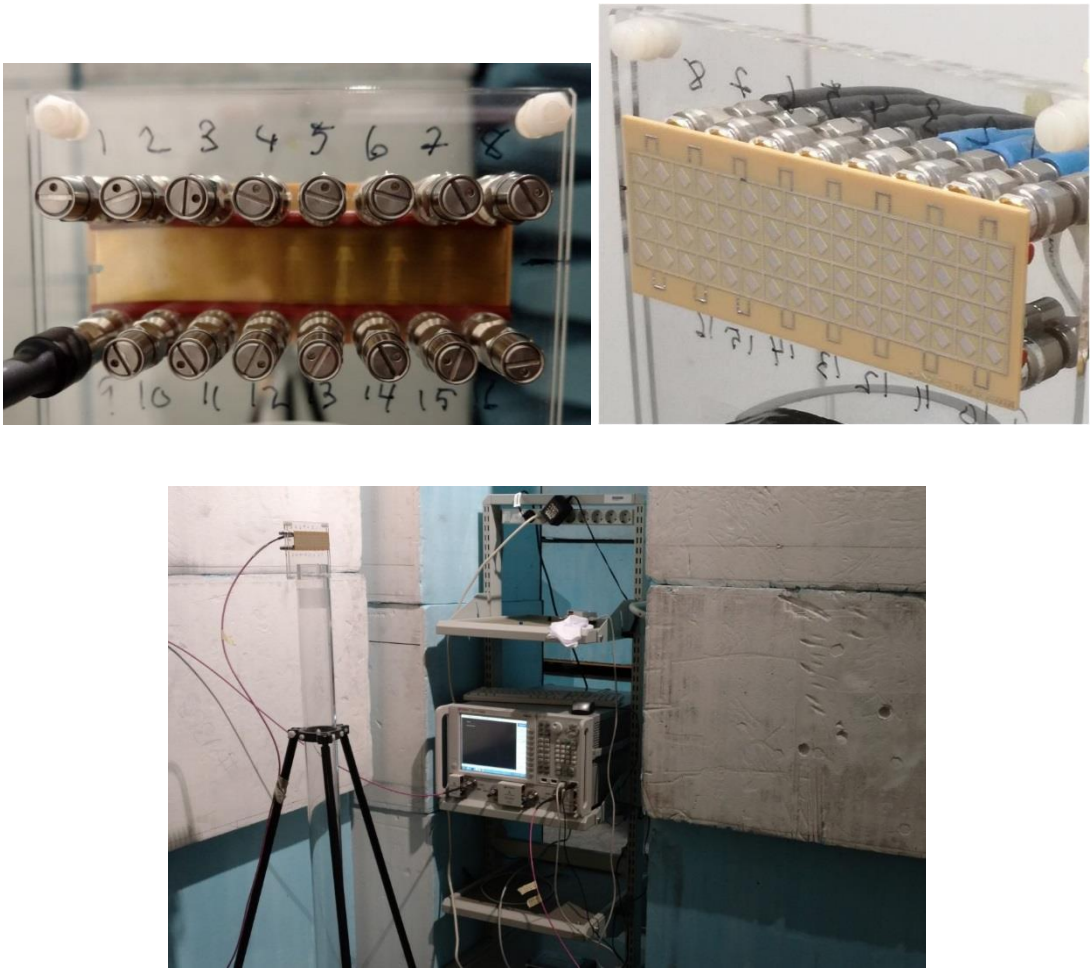

Figure 18: Radiation patterns measurements setup. The white are absorbing material.

4 Conclusions

The design, optimization and preliminary experimental results of the two antenna solutions, (i) electronically steerable transmitarray and (ii) electrically large phased array, developed in the 5GCHAMPION project and used to implement the backhaul have been presented in this report.

In the Section 2, the 1-bit linearly-polarized transmitarray with beam-steering capability has been presented. Firstly, the electronically tunable unit-cell architecture, optimization and characterization have been discussed. The unit-cell has been validated considering a waveguide simulator setup and it has been designed in order to cover the 25 – 29 GHz frequency band. The full transmitarray has also been designed and fabricated. It is composed of a 10-dBi standard gain horn as a focal source, a 400-element flat-lens array with 800 PIN diodes integrated on the unit-cells, and a steering logic board. The transmitarray has been simulated considering the ad-hoc simulation tool developed at CEA-Leti. The simulation results are very promising and demonstrate the possibility to steer the beam in a 2D window of 120°×120°. The transmitarray will be experimentally characterized and the results will be presented in the deliverable D3.3 (*Beamforming antennas and front-end integration*). The maximum gain is around 22.5 dBi in the broadside direction and higher than 17 dBi when the beam is steered at ±60°.

In the Section 3, the antenna architecture based on massive MIMO phased array has been presented. The array consists of sub-arrays, which each has 2×2 element patch antennas. The sub-array is linearly-polarized and each patch element are excited with the same amplitude and equal phase. The total number of patch antennas in the massive-MIMO beamforming matrix is 4×16 elements, meaning 2×8 sub-arrays, and totally 64 elements. The presented simulation and measurement results are based on the Version 1, and, thus, the goal of the -10 dB impedance bandwidth was set to the 26.65 – 27.50 GHz, whereas the final version, which will be used to implement the final backhaul link, will cover the bandwidth from 24.25 to 29.20 GHz including both ±45° polarization components. The radiation patterns are measured element by element and the results are summed in post-processing. Sidelobe level are 15 dB below the maximum gain which was predicted. The maximum gain is around 20 dBi as the theory is predicting max. 21.5 dBi so there is a good correlation between the results.

The possibility to integrate the two antenna solution, i.e. use the phase array as a focal source for the electronically steerable flat-lens array is under analysis.

References

[1] A. Clemente, L. Dussopt, R. Sauleau, P. Potier, and P. Pouliguen, “1-bit reconfigurable unit-cell based on PIN diodes for transmit-array application in X-band,” *IEEE Trans. Antennas Propag.*, vol. 60, no. 5, pp. 2260-2269, May 2012.

[2] A. Clemente, L. Dussopt, R. Sauleau, P. Potier, and P. Pouliguen, “Wideband 400-element electronically reconfigurable transmitarray in X band,” *IEEE Trans. Antennas Propag.*, vol. 61, no. 10, pp. 5017-5027, Oct. 2013.

[3] L. Di Palma, A. Clemente, L. Dussopt, R. Sauleau, P. Potier, and P. Pouliguen, “1-bit reconfigurable unit-cell for ka-band transmitarrays,” *IEEE Antennas Wireless Propag. Letters*, vol. 15, pp. 560-563, 2016.

[4] L. Di Palma, A. Clemente, L. Dussopt, R. Sauleau, P. Potier, and P. Pouliguen, “Circularly-polarized reconfigurable transmitarray in Ka-band with beam scanning and polarization switching capabilities,” *IEEE Trans. Antennas Propag.*, Vol. 65, no. 2, pp. 529-540, Feb. 2017.

[5] “MACOM Technologies,” [Online]. Available: http://www. macom.com.

[6] L. Di Palma, “Reconfigurable transmitarray antennas at millimeter wave frequencies,” PhD dissertation, Université Rennes 1, Dec. 2015.